Earthq Eng & Eng Vib (2012) 11: 43-55 **DOI**: 10.1007/s11803-012-0097-1

Performance-based semi-active control algorithm for protecting base isolated buildings from near-fault earthquakes

Behnam Mehrparvar[1†] and Taramarz Khoshnoudian[2§]

1. *Department of Civil Engineering, West Tehran Branch, Islamic Azad University, Tehran, Iran*

2. *Department of Civil Engineering, Amirkabir University of Technology, Tehran, Iran*

Abstract: Base isolated structures have been found to be at risk in near-fault regions as a result of long period pulses that may exist in near-source ground motions. Various control strategies, including passive, active and semi-active control systems, have been investigated to overcome this problem. This study focuses on the development of a semi-active control algorithm based on several performance levels anticipated from an isolated building during different levels of ground shaking corresponding to various earthquake hazard levels. The proposed performance-based algorithm is based on a modified version of the well-known semi-active skyhook control algorithm. The proposed control algorithm changes the control gain depending on the level of shaking imposed on the structure. The proposed control system has been evaluated using a series of analyses performed on a base isolated benchmark building subjected to seven pairs of scaled ground motion records. Simulation results show that the newly proposed algorithm is effective in improving the structural and nonstructural performance of the building for selected earthquakes.

Keywords: structural control; active control; semi-active control; base isolation

1 Introduction

Seismic base isolation is one of the most efficient systems available to protect building structures from the destructive effects of earthquakes, and has been broadly applied in various full-scale structures. The principal idea in base isolation is to reduce the seismic responses by inserting a relatively flexible layer between the foundation and the structure (Skinner *et al*., 1993). By doing this, the natural period and damping of the structure will be increased, which can reduce the responses of the superstructure, especially interstory drifts and floor accelerations (Naeim and Kelly, 1999). Alternatively, base displacements in those systems, especially under near-fault ground motions, are increased (Hall *et al*., 1995). The first concerns about this issue surfaced following the 1992 Landers earthquake and the 1994 Northridge earthquake, where long-period pulse-type ground motions were observed in near-fault records. Previous research has proven that earthquake records in near-field regions may have large energy in low frequencies and can cause huge responses in base isolated structures (Heaton *et al*., 1995). Conventional base isolation systems are equipped with passive energy-dissipating devices to decrease large isolator displacement demands enforced by rigorous code provisions in near-fault site locations. However, earlier studies have shown that heavy damping may increase superstructure accelerations and drifts (Jangid and Kelly, 2001; Kelly, 1999; Ariga *et al*., 2006; Makris and Chang, 1998). Different researchers have studied the possibility of solving this problem by using a hybrid control strategy that consists of a passive base isolation system and either an active or a semi-active control system (Yang and Agrawal, 2002; Erkus and Johnson, 2003; Johnson *et al*., 1998). Hybrid isolation systems were found to be very useful in enhancing both the structural and nonstructural performance of base isolated buildings subjected to strong earthquakes (Inaudi and Kelly, 1990; Nagarajaiah *et al*., 1993; Yang *et al*., 1996; Spencer *et al*., 1997; Gavin and Aldemir, 2005). Several advantages of active control systems over passive devices can be cited, such as enhanced effectiveness in response control, relative insensitivity to site conditions and ground motions, applicability to multi-hazard mitigation situations, and selectivity of control objectives. Nevertheless, the active control system requires a large external power supply for structural systems during seismic events, which along with reliability and other issues make them unsuitable for broad application in civil engineering. In contrast, semi-active control systems possess most of the advantages of active control systems without requiring large energy sources; however, they lack reliability (Chu *et al*., 2005). A significant amount of research has been completed on hybrid control of

Correspondence to: Behnam Mehrparvar, Department of Civil Engineering, West Tehran Branch, Islamic Azad University, Tehran, Iran
Tel: +98(21)88009966
E-mail: b_mehrparvar@wtiau.ac.ir
[†]Assistant Professor; [§]Associate Professor

Received March 13, 2011; **Accepted** November 14, 2011

structures by parallel use of base isolation and active or semi-active systems and the effectiveness of this method has been verified both in theory and practice. Most of this research has been performed on control algorithms used to calculate the control force of the devices. For example, Gavin and Aldemir (2005) studied optimal semi-active control method in addition to the pseudo-skyhook control algorithm and compared the two control strategies. Recently, the American Society of Civil Engineers (ASCE) structural control committee has developed a smart base isolated benchmark problem to systematically compare different control algorithms (Narasimhan *et al*., 2006). The degree of efficiency of each proposed algorithm in reducing the seismic responses of the benchmark building using seven pairs of near-fault ground motions was compared via several pre-defined performance indices. This paper proposes a new method of designing a semi-active control system based on the well-known skyhook control algorithm, which considers different performance levels. The performance-based control algorithm controls the responses of the base isolated benchmark building based on different performance levels required for different seismic hazard levels. The desired performances were achieved by changing the control gain of the modified skyhook control algorithm. The method presented in this paper for designing multi-performance control algorithms may be used to design active or semi-active structural control systems using other modern control algorithms.

2 Semi-active skyhook control algorithm

In this section, the required information for semi-active skyhook control of an isolation system is presented (Meirovitch, 1986).

Figure 1 shows a passive isolation system for a single-degree-of-freedom system. The transfer function of the passive isolation system can be described as (Karnopp, 1995):

$$\frac{X}{X_{\mathrm{g}}}=\frac{1+\mathrm{j}2\xi_{\mathrm{p}}(\frac{\omega}{\omega_{\mathrm{n}}})}{1-(\frac{\omega}{\omega_{\mathrm{n}}})^2+\mathrm{j}2\xi_{\mathrm{p}}(\frac{\omega}{\omega_{\mathrm{n}}})} \tag{1}$$

in which ξ_{p} is the passive damping ratio, ω_{n} and ω are the natural frequency of the system and the excitation frequency, and X, X_{g} are the displacements of the mass and the ground, respectively.

The plot of the transfer function in Eq. (1) versus $\omega/\omega_{\mathrm{n}}$ for various damping ratio values is shown in Fig. 2. Considering the transmissibility plot in Fig. 2, it is apparent that at low passive damping ratios, the transmissibility is relatively large around the resonant frequency (i.e., $\omega\approx\omega_{\mathrm{n}}$) and therefore provides poor isolation in this case. The enhancement of the damping value causes less transmissibility around resonant frequency while decreasing the isolation effect in the high-frequency excitations. Therefore, Fig. 2 indicates the trade-off between high-frequency and resonant isolation, which exists in passive damping mechanisms used for isolation systems. The skyhook control algorithm has been introduced to eliminate this trade-off in passive isolation systems. Moving the damper C to a position between the isolated mass M and an imaginary reference point in the sky, as demonstrated in Fig. 3, is the main idea of the skyhook control algorithm. Although such a reference point is unavailable in reality, the performance of such a configuration has been an interesting topic for researchers. The transfer function of this configuration may be stated as

$$\frac{X}{X_{\mathrm{g}}}=\frac{1}{1-(\frac{\omega}{\omega_{\mathrm{n}}})^2+\mathrm{j}2\xi_{\mathrm{sky}}(\frac{\omega}{\omega_{\mathrm{n}}})} \tag{2}$$

where ξ_{sky} represents the damping ratio of the ideal skyhook damper. Figure 4 illustrates the transmissibility as a function of $\omega/\omega_{\mathrm{n}}$ for different values of ξ_{sky}. Note that in this case, an increase in the skyhook damping ratio decreases the transmissibility for the entire range of frequencies, including high frequency excitations. Furthermore, note that with high skyhook damping ratios, i.e., above 0.707, isolation at resonant frequency is also achievable.

In practice, to provide an ideal skyhook control force in isolation systems, it is required to apply active force generators at the isolation level instead of passive

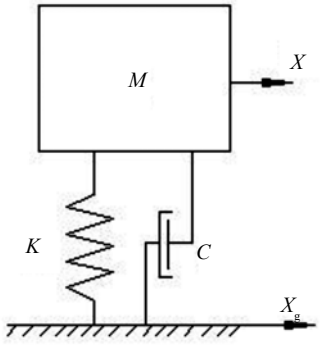

Fig. 1 Passive isolation diagram of a SDOF system

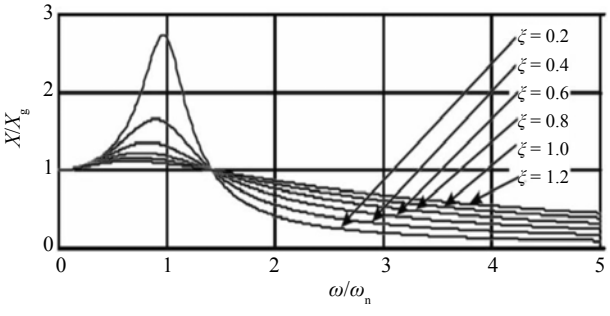

Fig. 2 Transfer function of a passive isolation system

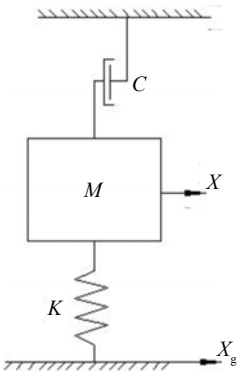

Fig. 3 Ideal skyhook damper configuration

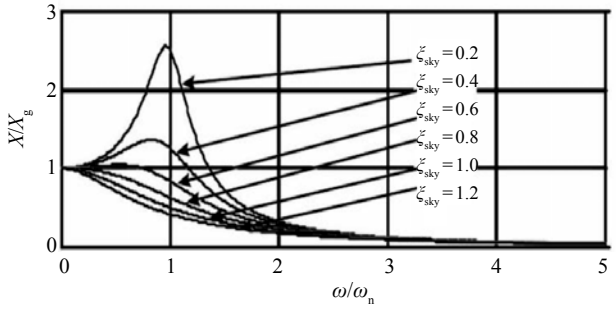

Fig. 4 Transfer function of the ideal skyhook damper system

dampers. In addition, it is possible to imitate the ideal skyhook force by means of semi-active dampers using semi-active skyhook control policies. Semi-active dampers provide variable damping force by changing the damping coefficient of the damper that requires a low level of power. The features of semi-active devices make them very efficient and reliable in view of the fact that they are not dependent on the main power sources that may be interrupted during earthquakes. Furthermore, in case of any malfunction in the controller system, they operate similar to passive dampers and do not cause instability problems. To simulate skyhook control force by semi-active dampers, the relative velocity across the damper is defined by:

$$V_{rel} = V_{abs} - V_g \tag{3}$$

where V_{abs} is the absolute velocity of the isolated mass, M. Therefore, the ideal skyhook damping force can be represented by:

$$F_{sky} = -C_{sky} V_{abs} \tag{4}$$

However, the semi-active damper can only produce a dissipative force at the opposite direction of the relative velocity across the damper. That is, the semi-active damping force is always equal to:

$$F_{sa} = -C_{sa} \cdot V_{rel} \tag{5}$$

where C_{sa} is the variable damping coefficient of the semi-active damper. Equation (5) states that the semi-active damper is able to imitate the ideal skyhook damping force when the absolute and relative velocities of the damper are in the same direction. Therefore, in order to adjust the semi-active damper to produce a damping force equal to the ideal skyhook damper, the damping coefficient should be changed according to the following equation:

$$C_{sa} = \frac{C_{sky} V_{abs}}{V_{rel}} \tag{6}$$

Consequently, the semi-active skyhook control rule can be stated by the following equations (Crosby *et al.*, 1973):

$$F_{sa} = \begin{cases} -C_{sky} V_{abs} & V_{abs} \cdot V_{rel} \geq 0 \\ 0 & V_{abs} \cdot V_{rel} < 0 \end{cases} \tag{7}$$

$$C_{sa} = \begin{cases} \dfrac{C_{sky} \cdot V_{abs}}{V_{rel}} & V_{abs} \cdot V_{rel} \geq 0 \\ 0 & V_{abs} \cdot V_{rel} < 0 \end{cases} \tag{8}$$

Thus, the term $V_{abs} \cdot V_{rel}$ is the controlling function for switching the semi-active damper from off to on and vice versa. Taking into consideration the maximum and minimum limits of the damping coefficient of semi-active dampers that exist in practice, the skyhook control rule is revised as:

$$C_{sa} = \begin{cases} \max\left[c_{min}, \min\left[\dfrac{C_{sky} V_{abs}}{V_{rel}}, c_{max} \right] \right] & V_{abs} \cdot V_{rel} \geq 0 \\ 0 & V_{abs} \cdot V_{rel} < 0 \end{cases} \tag{9}$$

3 Modified skyhook control algorithm

The conventional semi-active skyhook algorithm has the possibility to be improved. As a result of sudden changes in the damping force at the times of switching, the structure experiences a significant jerk that decreases the efficiency of the semi-active skyhook algorithm. Miller and Nobles (1990) studied this problem for an automobile suspension system and suggested that the damping force may be reduced at the low velocity region of the damper. This causes a gradual change in the damping force and it has been proven to be effective in jerk control. However, in this paper, the no-jerk skyhook control algorithm proposed by Ahmadian *et al.,* (2000) is used. This algorithm uses a shaping function to smooth the skyhook damping force. Note that the term $V_{abs} \cdot V_{rel}$ determines the switching instances of the semi-active damper. Therefore, two types of switching can be identified in the behavior of semi-active dampers as shown in Fig. 5: one is related to the changing of the relative velocity sign and the other to the changing of the absolute velocity sign.

It is obvious from Fig. 5 that at absolute velocity switches, the damping force increases according to

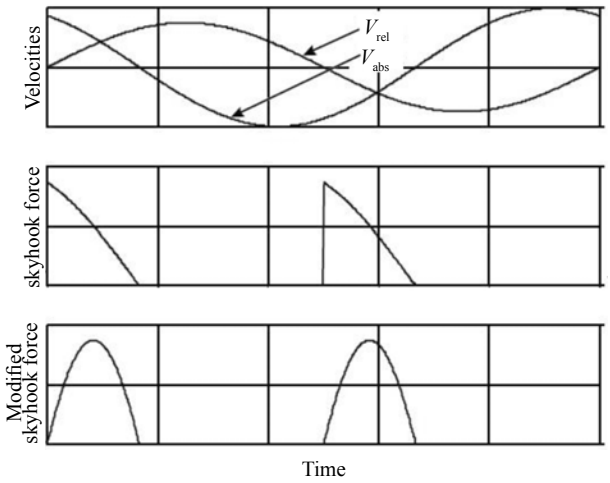

Fig. 5 Modification of skyhook damping force

the skyhook gain, C_{sky}. However, at relative velocity switches, the damping force rapidly increases and may therefore cause a jerk in the system. The no-jerk skyhook control algorithm eliminates this problem by multiplying a shaping function into the skyhook formula in order to remove the force discontinuity associated with relative velocity switches. The modified no-jerk skyhook control algorithm is stated by

$$F_{sa} = \begin{cases} -C_{sky} \cdot V_{abs} \cdot |V_{rel}| & V_{abs} \cdot V_{rel} \geq 0 \\ 0 & V_{abs} \cdot V_{rel} < 0 \end{cases} \quad (10)$$

In this control algorithm, the damping force is a function of both the relative and absolute velocities. Since in all of the switching times either the relative velocity or absolute velocity across the damper is zero, the control force changes gradually, thus eliminating the jerk problem caused by the relative velocity switches.

4 Base isolated building model

The base isolated building considered for the evaluations is similar to the benchmark base isolated building problem that has been developed by the ASCE structural control committee. The benchmark building is an eight-story steel frame building similar to existing buildings in Los Angeles, California (Narasimhan *et al*., 2006). The superstructure is modeled linearly and with rigid floor diaphragms. Consequently, the degrees of freedom are limited to three in each story. Therefore, the entire superstructure and the base are modeled by 27 degrees of freedom. The fundamental periods of the fixed base superstructure are 0.78 s, 0.89 s, and 0.66 s in the north-south direction, east-west direction, and rotation, respectively. The superstructure damping ratio is considered to be equal to 5% for all structural modes in the analyses. The selected isolation system consists of 92 similar linear elastomeric bearings located between the base slab and the footings. The plan of the benchmark building model is shown in Fig. 6. The stiffness and damping quantities of the linear isolators have been set to attain a natural period equal to 3.0 s and a damping ratio equal to 10% of critical damping for the entire isolation system. Furthermore, a semi-active control system, consisting of 16 semi-active dampers (eight dampers in each direction), has been added to the passive system to form the hybrid control system of the benchmark building. The dampers are capable of producing a variable damping force of up to 250 t and are controlled by a semi-active control algorithm as described in the next section.

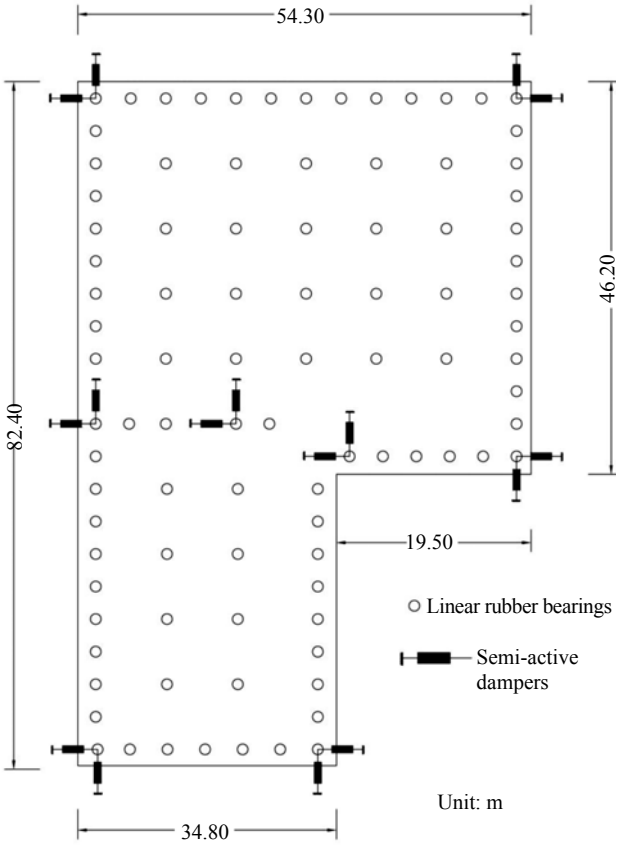

Fig. 6 Plan of the base isolated building model

5 Performance-based skyhook control algorithm

The modified skyhook control algorithm is a simple and efficient control strategy for protecting base isolated structures from earthquake ground motions. The only responses used as feedback for the controller are velocities across the semi-active dampers. Therefore, the dampers are self-controlled in the sense that they are only using their own local measurements, which make the control system very simple. Furthermore, the algorithm is a non-model based control policy, so that it can be easily applied to nonlinear plants where it is complicated to use common model-based control policies such as optimal control algorithms. In this algorithm, the only

parameter to be adjusted is the skyhook gain C_{sky}. Hence, it is possible to achieve different control objectives by adjusting this parameter. In order to calibrate the gain of the skyhook algorithm, a sensitivity analysis is required. In this paper, the control algorithm is tuned for three levels of earthquake ground motions. That is, the control system modifies the response of the base isolated building differently under very strong, strong and moderate earthquakes. These three earthquake levels are referred to as the Maximum Considered Earthquake (MCE), Design Basis Earthquake (DBE) and Service Earthquake (SE) levels, respectively.

For very strong ground motions (MCE), the most important responses to be controlled are the displacements of the isolators. Previous studies have proven that very strong earthquakes may lead to excessive displacements at the base level, which may result in the collision of the structure with adjacent barriers or cause failure of the isolators, both of which could end in total collapse of the base isolated building (Hall *et al*., 1995). Considering these two important issues, drift and acceleration response control will be of less significance in view of the fact that these responses in base isolated structures are relatively low compared with conventional fixed base structures and do not raise concern about the total collapse of the building. Therefore, it is rational for the control system to focus on reducing the responses of the isolators during a very strong event and, in this case, drift and floor acceleration responses are less important.

The next earthquake level to be considered is the DBE level, which relates to a strong earthquake event in which the deflections of the isolators are expected to be less than their capacity and also less than the size of the gap existing between the isolated building and their neighboring structures. In this earthquake level, reducing the deflections of the isolators does not make sense as the displacements neither cause an impact between the isolated building and other barriers nor results in the failure of the isolators. On the other hand, the most considerable responses at this level of ground motions are interstory drifts that can cause structural and nonstructural damage in the building. Seismic isolated structures are designed to behave linearly during the design earthquake. Therefore, at DBE level earthquakes, the control system tries to minimize the interstory drifts of the seismic isolated building by properly adjusting the skyhook gain of the system. This will result in a nearly elastic behavior of the structure and furthermore reduces the damage to nonstructural components.

Finally, at the service level earthquake, neither the displacements of the isolators nor interstory drifts are regarded as crucial responses. That is because the displacements of the isolators are too negligible to produce damage in the system; moreover the drifts are small enough for the structure to remain within the elastic limit. Therefore, the structural performance of the system is acceptable for a service earthquake level and the only concern may be about very sensitive nonstructural components, which are vulnerable at a certain level of accelerations. It is apparent that engineers have now well recognized the importance of nonstructural elements that are installed on the floors of important buildings. Keeping these systems operational after the occurrence of an earthquake is essential in making emergency services available. At present, the key parameters for evaluating the performance of nonstructural components are maximum floor accelerations and root mean square (RMS) of floor accelerations. For this reason, the control system focuses on controlling maximum floor acceleration responses in moderate level earthquakes.

6 Earthquake ground motions

Seven pairs of earthquake records related to different earthquakes cited in Table 1 have been used to evaluate the benchmark building model. The ground motion records selected are exactly the same as those used in the smart base isolated benchmark problem defined by the ASCE structural control committee and all of them have been identified as having distinct velocity pulses. Figure 7 illustrates both acceleration components of the selected records (PEER). The records have been scaled to represent three earthquake levels corresponding to Maximum Considered Earthquake (MCE), Design Basis Earthquake (DBE) and Service Earthquake (SE) events.

The scaling process is based on the acceleration response spectra of the selected records. For this

Table 1 Characteristics of selected earthquake ground motions

Earthquake	Station	PGA (g)	PGV(cm/s)	T_p(s)
Northridge, USA 1994/01/17	Sylmar	0.88	129	2.6
Northridge, USA 1994/01/17	Rinaldi	0.84	160	1.05
Northridge, USA 1994/01/17	Newhall	0.74	117	1.25
Kobe, Japan 1995/01/16	KJMA	0.84	92	0.85
Chi-Chi, Chinese Taiwan 1999/09/20	Jiji	0.51	265	9.0
Erzincan, Turkey 1992/03/13	Erzincan	0.51	82	2.2
Imperial Valley, USA 1979/10/15	El Centro	0.31	30	3.0

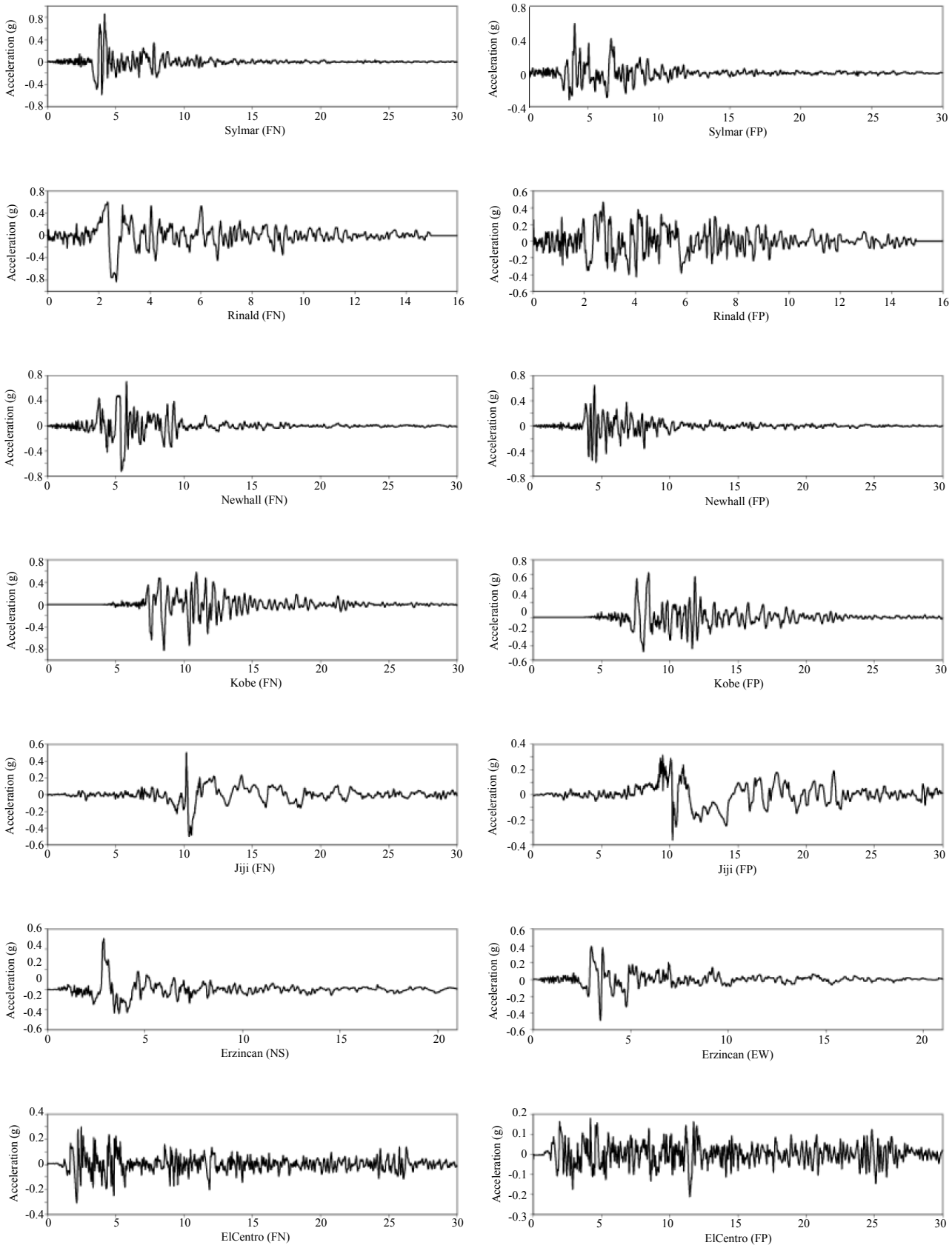

Fig. 7 Acceleration time-histories of selected earthquake records

Table 2 Earthquake records scale factors

Earthquake record	MCE scale factor	DBE scale factor	SE scale factor
Newhall	1.68	1.12	0.29
Sylmar	1.55	1.04	0.27
ElCentro	3.58	2.39	0.60
Rinaldi	1.53	1.02	0.26
Kobe	2.04	1.36	0.35
Jiji	0.66	0.44	0.12
Erzincan	1.37	0.92	0.24

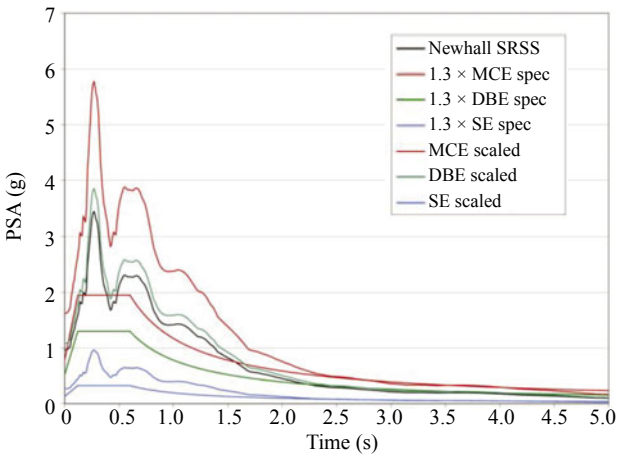

Fig. 8 Original and scaled response spectra of Newhall record

purpose, the seismic parameters of the three seismic levels are taken as:

MCE spectral accel. at short periods $S_{MS} = 1.5$ g

MCE spectral accel. at 1 s period $S_{M1} = 0.9$ g

DBE spectral accel. at short periods $S_{DS} = \frac{2}{3} S_{MS} = 1.0$ g

DBE spectral accel. at 1s period 0.6g $S_{D1} = \frac{2}{3} S_{M1} = 0.6$ g

SE spectral accel. at short periods $S_{SS} = \frac{1}{4} S_{DS} = 0.25$ g

SE spectral accel. at 1s period $S_{S1} = \frac{1}{4} S_{D1} = 0.15$ g

For each pair of horizontal ground-motion components, the square root of sum of the squares (SRSS) of the 5% damped spectra of the horizontal components was constructed. The motions have been scaled such that the SRSS spectra for each earthquake record does not fall below 1.3 times the 5% damped spectrum of the maximum, design or service earthquake by more than 10% for periods between $0.5T$ and $1.25T$ where T is the natural period of the isolation system. Therefore, for each record, three scale factors corresponding to the three considered earthquake levels were calculated and tabulated (Table 2). Moreover, as an example, the original and scaled spectra for the Newhall record are demonstrated in Fig. 8.

In this study, the two components of the records were applied simultaneously to the models for evaluation purposes.

7 Numerical simulations and results

The mathematical model of the benchmark base isolated building in conjunction with the controller system has been analyzed for the selected earthquake records using MATLAB and SIMULINK (MATLAB, 2000). In order to calibrate the skyhook control gain for different performance objectives, a sensitivity analysis was carried out. The maximum responses for base displacements, interstory drifts and floor accelerations were calculated for a range of C_{sky} values under the scaled ground motions. Figures 9–11 demonstrate the plots of the maximum responses against skyhook gain, C_{sky} , for three seismic levels to be considered in the controller design.

From Figs. 9–11, note that an increase in the gain value always makes a decrease in maximum base displacement quantities. Therefore, for the sole purpose of controlling the base displacements, the skyhook gain will be set as large as possible. However, the analyses results illustrate that increasing this parameter beyond a certain level have a very small effect. Consequently, as illustrated in Fig. 9 for very strong ground motions (MCE event), where the major concern is about excessive isolator displacements, the skyhook gain is set equal to 25,000 kN·s/m. This will cause the maximum skyhook damping to minimize the displacement of the isolators at the base level, but it will also slightly increase interstory drifts and floor accelerations as demonstrated in Fig. 9. However, this increase in drift and acceleration responses will be allowed, since the building may sustain more severe damage due to extreme deflections in the isolators than due to large interstory drifts or floor accelerations.

Figure 10 shows the maximum responses corresponding to the DBE scaled earthquake records for various values of the C_{sky} parameter. At this earthquake level, the base displacements can easily be controlled to less than 40 cm, which is within the working range of common isolators in use today. Furthermore, since the size of the moat width, which defines the zone of free movement for an isolated structure, has often been larger than 40 cm in previous completed projects (Hall *et al*., 1995) it is impossible for impact between the building and other barriers to occur. Thus, at this level, in which the damage to the building is mostly due to the drifts

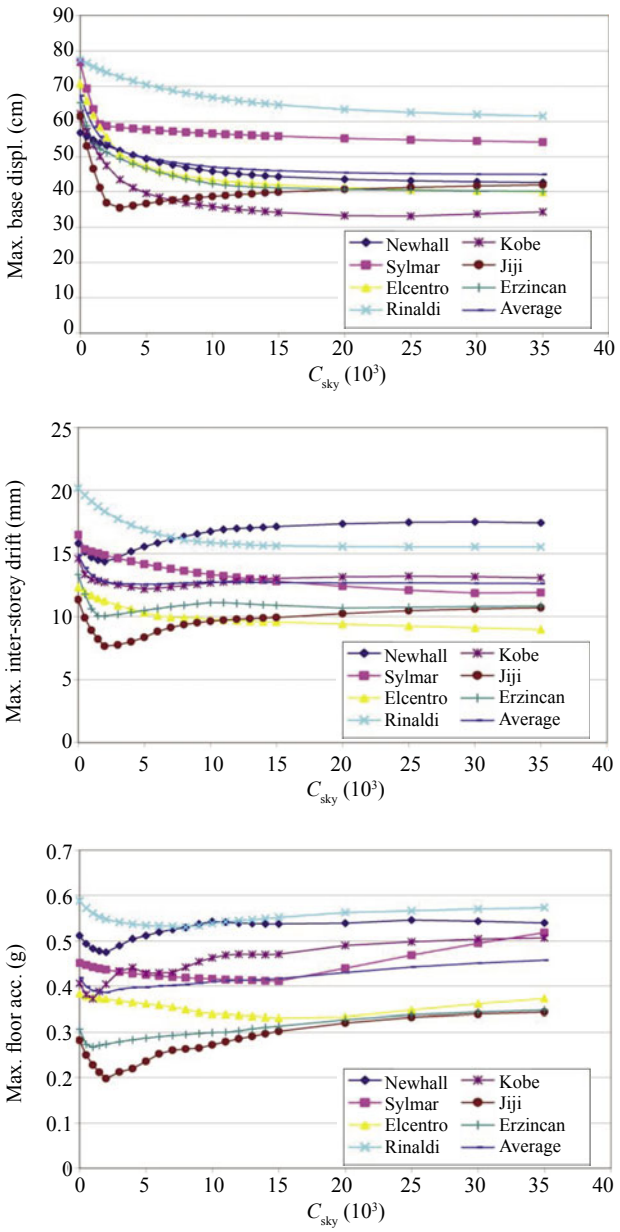

Fig. 9 Maximum responses for MCE scaled records

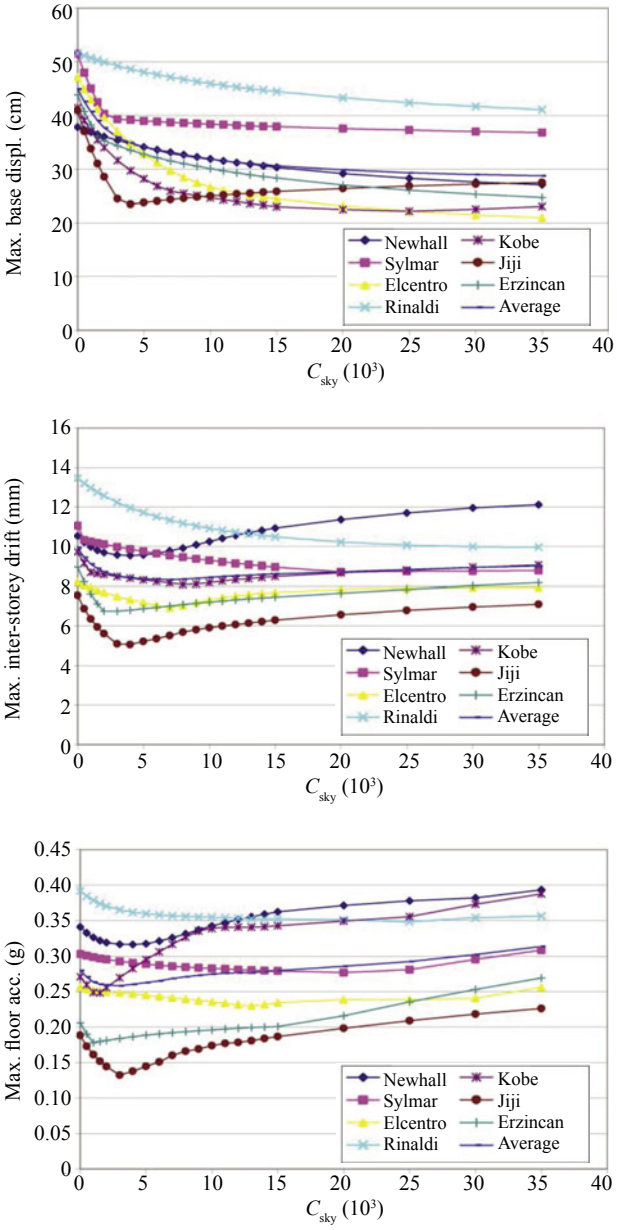

Fig. 10 Maximum responses for DBE scaled records

caused by the earthquake, the controller gain will be set to a value to produce minimum drifts in the building. As illustrated in Fig. 10 the minimum interstory drifts based on the average of the results are produced by the value of C_{sky}=7000 kN·s/m while maximum base displacement can be adequately controlled. Thus, for base displacements above a certain value that characterizes a DBE event the skyhook gain is adjusted equal to this quantity.

Also at the moderate earthquake level, where no damage resulting from the displacements of the isolators or interstory drifts occurs, the controller minimizes absolute accelerations of the floors in order to improve nonstructural performance of the building. Figure 11 shows that this can be done by a value of C_{sky} equal to 5000 kN·s/m while the interstory drifts keep the structure within the elastic limit. Thus, the proposed performance-based skyhook control algorithm may be written as:

$$F_{sa}=\begin{cases}\begin{cases}C_{sky}^{M}V_{abs}\cdot|V_{rel}| & V_{abs}\cdot V_{rel}\geq 0\\ 0 & V_{abs}\cdot V_{rel}<0\end{cases} & d_D\leq D\\ \begin{cases}C_{sky}^{D}V_{abs}\cdot|V_{rel}| & V_{abs}\cdot V_{rel}\geq 0\\ 0 & V_{abs}\cdot V_{rel}<0\end{cases} & d_S\leq D<d_D\\ \begin{cases}C_{sky}^{S}V_{abs}\cdot|V_{rel}| & V_{abs}\cdot V_{rel}\geq 0\\ 0 & V_{abs}\cdot V_{rel}<0\end{cases} & D<d_S\end{cases} \tag{11}$$

or in terms of variable damping value

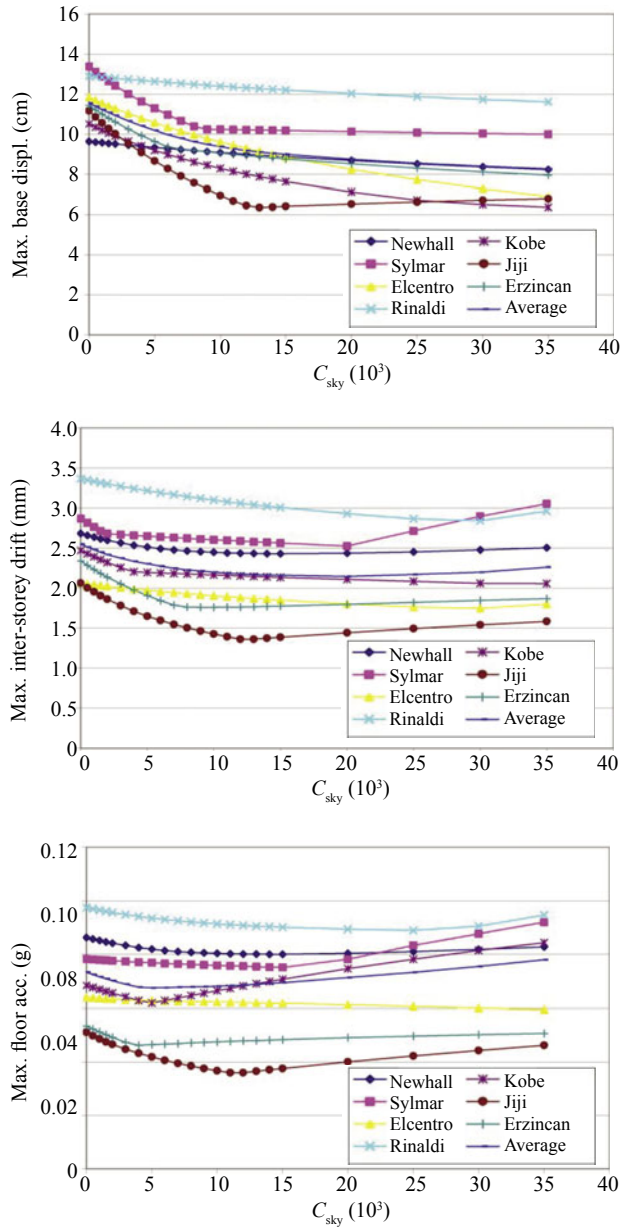

Fig. 11 Maximum responses for SE scaled records

$$C_{sa}=\begin{cases}\begin{cases}\max\left[C_{min},\min\left[C_{sky}^{M}|V_{abs}|,C_{max}\right]\right] & V_{abs}\cdot V_{rel}\geq 0\\ C_{min} & V_{abs}\cdot V_{rel}<0\end{cases} & d_D\leq D\\ \begin{cases}\max\left[C_{min},\min\left[C_{sky}^{D}|V_{abs}|,C_{max}\right]\right] & V_{abs}\cdot V_{rel}\geq 0\\ C_{min} & V_{abs}\cdot V_{rel}<0\end{cases} & d_S\leq D<d_D\\ \begin{cases}\max\left[C_{min},\min\left[C_{sky}^{S}|V_{abs}|,C_{max}\right]\right] & V_{abs}\cdot V_{rel}\geq 0\\ C_{min} & V_{abs}\cdot V_{rel}<0\end{cases} & D<d_S\end{cases} \quad (12)$$

where

$C_{sky}^{S}=5000$ kN.s/m

$C_{sky}^{D}=7000$ kN.s/m

$C_{sky}^{M}=25000$ kN.s/m

The values of d_S and d_D, the margins which define the MCE, DBE and SE working range of the proposed control algorithm, are selected by a trial and error process to obtain the quantities that result in the best performance of the algorithm. After performing such analyses, the following values are suggested for these parameters.

$$d_S=11\text{ cm}$$

$$d_D=36\text{ cm}$$

Figure 12 illustrates the time-histories of the base displacement and top floor acceleration of the controlled and uncontrolled structures in X direction under the MCE scaled Newhall record. Also in this figure the variation of skyhook gain C_{sky} during the time is presented accompanied by the time-history of the control force

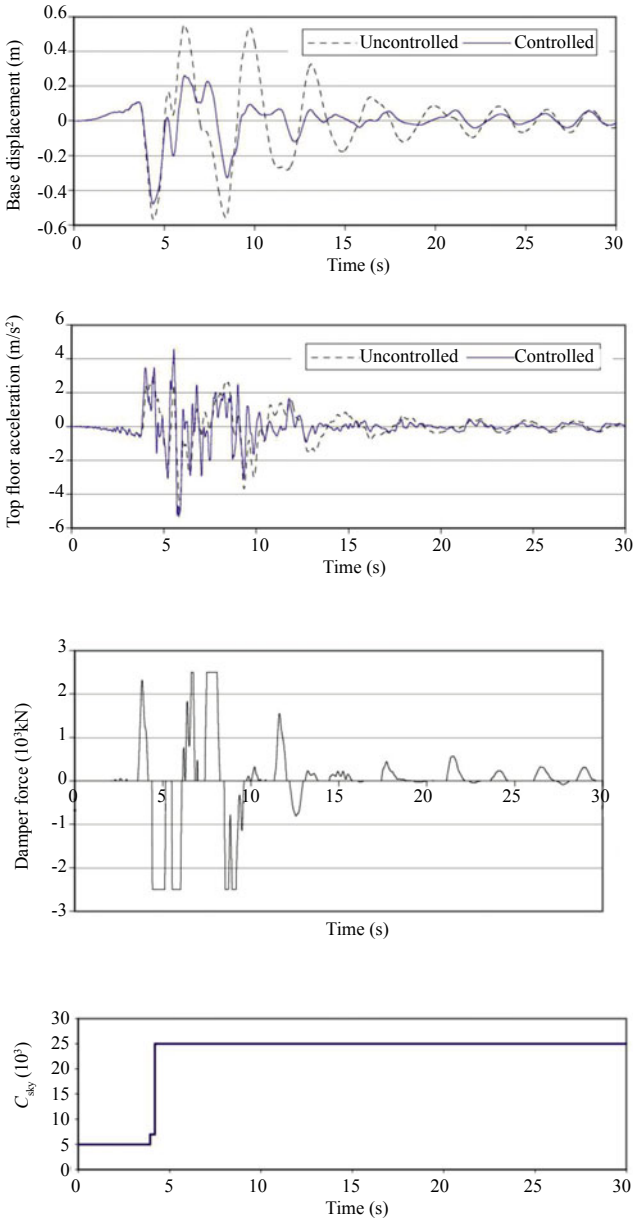

Fig. 12 Time-histories of the responses and control force under MCE scaled Newhall record

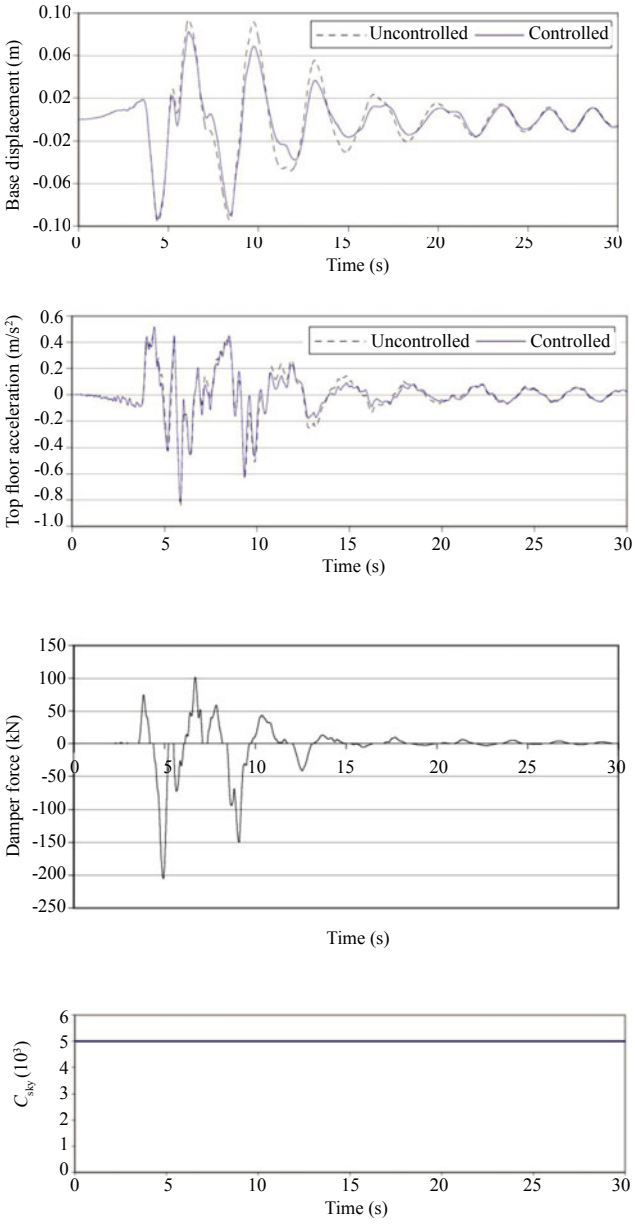

Fig 13 Time-histories of the responses and control force under SE scaled Newhall record

related to one of the dampers located in the *X* direction. Note that after the first minor shakings of the earthquake, the gain value has increased to 25,000 kN·s/m to decrease the displacements of the isolators as much as possible. Although this has resulted in rapid changes in the control force at the switching times, which cause some jerks in the acceleration response of the building, the jerks can be ignored at this stage because of the priority of the decrease in base displacements.

In Fig. 13, the same time-histories are presented for the SE scaled Newhall record. In this figure, it is notable that the gain value remains equal to 5000 kN·s/m due to the small base displacements caused by this record. For this record, the control force variations at the switching instances are more gradual, which reduces the jerks in the acceleration responses. However, it only poorly controls the base displacements that are not major issues for moderate earthquakes. Therefore, it can be seen how the performance-based algorithm controls different responses with regard to the importance of each response at different seismic events.

Tables 3–5 represent the maximum responses of the proposed control algorithm for the selected earthquake records scaled for different seismic levels.

In order to evaluate the results of the proposed control algorithm, the uncontrolled model was also analyzed for a range of passive damping values. Figures 14–16 demonstrate the peak responses of the displacements of the isolators, interstory drifts, and floor accelerations of the passively controlled structures under the three levels of earthquake motions. It has been pointed out that conventionally, isolated structures are controlled passively by adding dampers to the isolation system. A comparison between the responses attained through the passive control system and the results of the proposed semi-active algorithm demonstrates the efficiency of the semi-active control system with respect to the passive control strategy.

A comparison between the average of the maximum base displacement results for MCE scaled records (48.4 cm) and the results of the passively controlled

Table 3 Results of the proposed control algorithm under MCE scaled records

	Newhall	Sylmar	ElCentro	Rinaldi	Kobe	Jiji	Erzincan	Average
Max. base displacement (cm)	47.8	57.9	45.1	68.9	36.8	37.5	44.5	48.4
Max. interstory drift (mm)	17.7	14.1	10.0	16.3	12.4	9.3	11.1	13.0
Max. floor acceleration (g)	0.54	0.46	0.37	0.56	0.43	0.26	0.35	0.43

Table 4 Results of the proposed control algorithm under DBE scaled records

	Newhall	Sylmar	ElCentro	Rinaldi	Kobe	Jiji	Erzincan	Average
Max. base displacement (cm)	33.9	39.1	29.7	47.7	25.9	24.3	31.5	33.2
Max. interstory drift (mm)	10.2	9.7	6.9	11.5	8.2	5.5	7.0	8.4
Max. floor acceleration (g)	0.34	0.29	0.24	0.38	0.32	0.16	0.19	0.28

Table 5 Results of the proposed control algorithm under SE scaled records

	Newhall	Sylmar	ElCentro	Rinaldi	Kobe	Jiji	Erzincan	Average
Max. base displacement (cm)	9.3	11.1	10.6	12.6	9.2	8.6	9.6	10.1
Max. interstory drift (mm)	2.5	2.6	2.0	3.2	2.2	1.7	1.9	2.3
Max. floor acceleration (g)	0.08	0.08	0.06	0.09	0.06	0.04	0.05	0.07

structures presented in Fig. 14 shows that decreasing the average base displacement to this level by passive control technique requires augmenting the damping ratio of the isolation system to more than 30% of the critical value. However, this figure also shows that this level of damping will cause an average maximum interstory drift and floor acceleration equal to 18 mm and 0.56 g, respectively, for the average of seven selected records compared with 13 mm and 0.43 g, which were produced by the proposed semi-active system.

Also for DBE scaled records, Fig. 15 shows that the optimum damping value for minimizing interstory drifts of the structure is equal to 15% of the critical value based on the average of the results, which produces

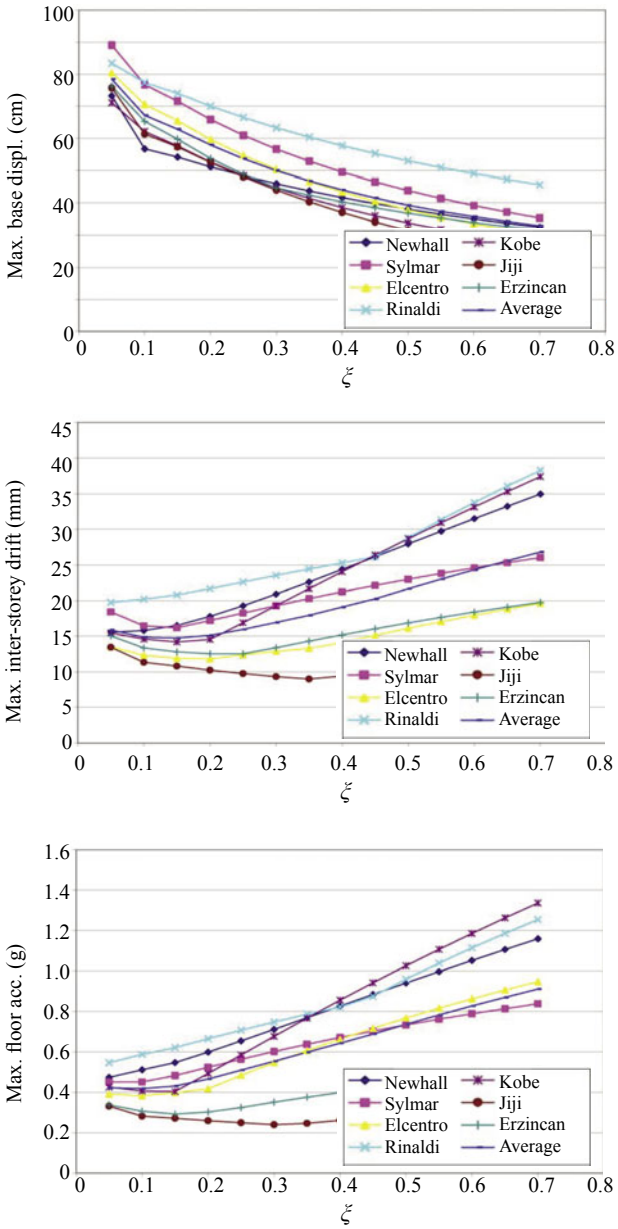

Fig. 14 Maximum responses vs. damping for uncontrolled models under MCE scaled records

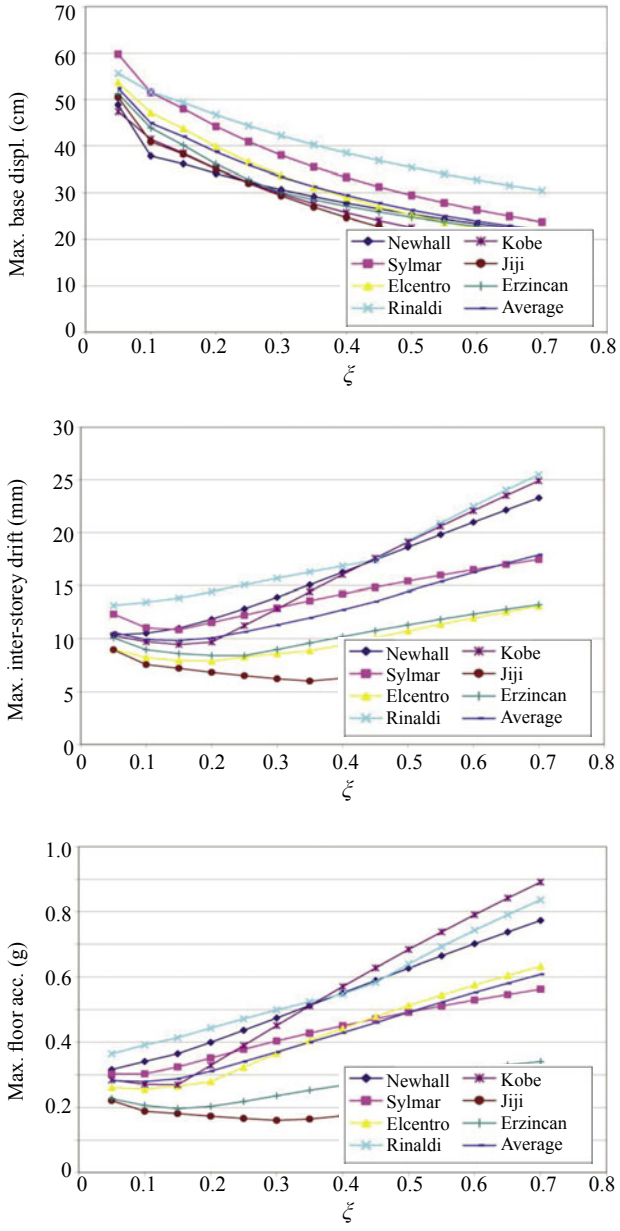

Fig. 15 Maximum responses vs. damping for uncontrolled models under DBE scaled records

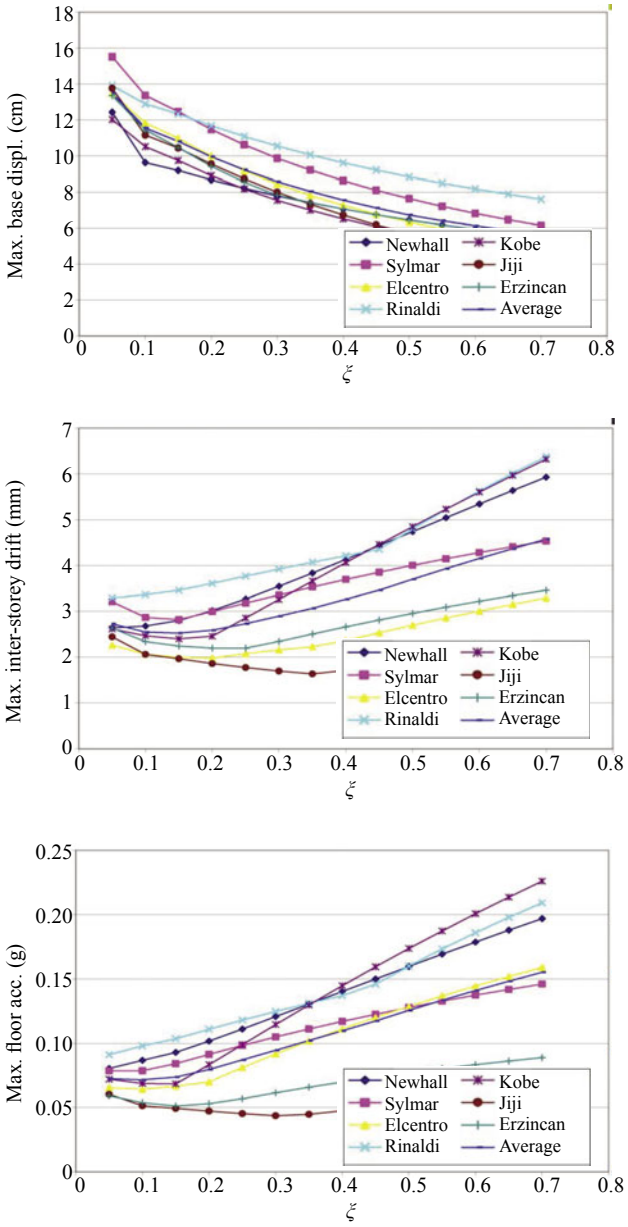

Fig. 16 Maximum responses vs. damping for uncontrolled models under SE scaled records

a maximum drift equal to 9.8 mm and a maximum floor acceleration equal to 0.29 g while reducing the maximum base displacement of the building to 42 cm. Again, comparing these responses with those in Table 4 proves the efficiency of the proposed semi-active control algorithm, even with respect to a passive system with the optimal choice of damping.

Figure 16 corresponds to the service earthquake responses. In this figure the optimal damping ratios for minimizing drifts and accelerations are 15% and 10%, respectively. Comparing the results corresponding to these damping ratios with those of the proposed algorithm tabulated in Table 5 once again verifies the efficacy of the proposed control system.

Moreover, the results of the performance-based skyhook control system show a better performance with regard to the conventional skyhook control system, as shown in Figs. 9–11, considering the fact that the controller focuses on reducing key responses at different earthquake levels.

The near-fault parameters, i.e., pulse period (T_p) and pulse velocity (V_p), for the selected ground motions are also given in Table 1. It shows that the records have a variety of values for these two parameters. It is obvious in Figs. 9–11 that the records with the highest V_p values caused the largest responses in the base isolated structure taking into account the scale factors applied in the records. However, except for the Rinaldi and Sylmar records, the controlling effect of the semi-active control system is almost the same for all the other recorded ground motions. The reduction in the responses corresponding to the Rinaldi and Sylmar records is somewhat less when compared to the other records. This observation could be related to the pulse period of these records, which is about 1 s for both. However, the semi-active control system is still effective for all the near-field records, which cover a wide range of magnitudes for T_p and V_p parameters. Therefore, the proposed control system could be used efficiently for base isolated structures in different near-fault zones.

8 Conclusions

This paper presents a performance-based semi-active control system to improve the seismic performance of base isolated buildings. The control algorithm is based on the modified no-jerk skyhook algorithm and the controller gain is adjusted based on the ground motion level applied to the system. The goal of the controller is to reduce the different responses of the structure based on the degree of the intensity of the applied ground motions. The efficiency of the proposed algorithm was evaluated by seven pairs of ground motions scaled at three different earthquake levels. The peak responses of the controlled structure including base displacements, interstory drifts and floor accelerations were computed via computer simulations under the selected records. Evaluation of the results shows that the proposed algorithm can be much more efficient than passive control strategies (i.e., adding damping to the isolation system), while also has the simplicity of the well-known skyhook control algorithm that makes it easy to use in complex structural systems. Furthermore, the benefits of the performance-based algorithm over the conventional skyhook method were proven both in jerk reduction and controlling different responses based on the level of ground shakings. The results showed that the proposed control system can cause a decrease in all the responses, i.e., maximum base displacement, maximum interstory drift and maximum floor acceleration, in the benchmark building under near-fault ground motions, simultaneously. The paper also presents the concept of designing a semi-active controller system based on

various performance levels anticipated from a base isolated building. The performance-based control concept, which was applied to the no-jerk skyhook control algorithm in this paper, could be extended to other control strategies and other types of structures in future studies.

References

Ahmadian M, Brian R and Song X (2000), *No-Jerk Semi-Active Skyhook Control Method and Apparatus*, United States Patent, USA.

Ariga T, Kanno Y and Takewaki I (2006), "Resonant Behavior of Base-isolated High-rise Buildings Under Long-period Ground Motions," *The Structural Design of Tall and Special Building,* **15**: 325–338.

Chu SY, Soong TT and Reinhorn AM (2005), *Active, Hybrid, and Semi-active Structural Control*, *A Design and Implementation Handbook*, John Wiley & Sons: New York, USA.

Crosby MJ, Karnopp D, *et al*. (1973), "Vibration Control Using Semi-active Force Generators," *Transactions of the ASME* , Paper 73-DET-122.

Erkus B and Johnson EA (2003), "Benchmark Base Isolated Building with Controlled Bilinear Isolation," *Proceedings of the 16th ASCE Engineering Mechanics Conference*.

Gavin HP and Aldemir U (2005), "Optimal Control of Earthquake Response Using Semi-active Isolation," *Journal of Engineering Mechanics*, ASCE, 769–776.

Hall JH, Heaton TH, Halling MW and Wald DJ (1995), "Near-source Ground Motion and Its Effect on Flexible Buildings," *Earthquake Spectra*, **11**: 569–605.

Heaton TH, Hall JH, Wald DJ and Halling MW (1995), "Response of High-rise and Base-isolated Buildings in a Hypothetical M_W 7.0 Blind Thrust Earthquake," *Science*, **267**: 206–211.

Inaudi JA and Kelly JM (1990), "Active Isolation," *U.S. National Workshop on Structural Control Research*, Los Angeles, 125–130.

Jangid RS and Kelly JM (2001), "Base Isolation for Near-Fault Motions," *Earthquake Engineering and Structural Dynamics*, **30**: 691–707.

Johnson EA, Ramallo JC, Spencer BF and Sain MK (1998), "Intelligent Base Isolation Systems," *Proceedings of the 2nd World Conference on Structural Control*, Kyoto, Japan.

Karnopp D (1995), "Active and Semi-active Vibration Isolation," *Journal of Vibrations and Acoustics*, **117**(3B): 177–185.

Kelly JM (1999), "The Role of Damping in Seismic Isolation," *Earthquake Engineering and Structural Dynamics*, **28**: 3–20.

Makris N and Chang SP (1998), "Effect of Damping Mechanisms on the Response of Seismically Isolated Structures," *Report No. PEER-98/06*, University of California, Berkeley, CA.

MATLAB (2000), The Math Works, Inc.

Meirovitch L (1986), *Elements of Vibration Analysis*, McGraw-Hill, Inc., New York.

Miller LR and Nobles CM (1990), Methods for Eliminating Jerk and Noise in Semi-active Suspensions, SAE Trans., SAE paper.

Naeim F and Kelly JM (1999), *Design of Seismic Isolated Structures, from Theory to Practice*, John Wiley & Sons: New York, USA.

Nagarajaiah S, Riley MA and Reinhorn A (1993), "Control of Sliding-isolated Bridge with Absolute Acceleration Feedback," *Journal of. Eng. Mech.,* **119**(11): 2317–2332.

Narasimhan S, Nagarajaiah S, Johnson EA and Gavin HP (2006), "Smart Base-isolated Benchmark Building Part I: Problem Definition," *Journal of Structural Control and Health Monitoring,* **13**: 573–588.

PEER (Pacific Earthquake Engineering Research Center) Strong Motion Database. University of California, Berkeley; http://peer.berkeley.edu

Skinner RI, Robinson WH, and McVerry GH, *An Introduction to Seismic Isolation,* Wiley, Chichester, England, 1993.

Spencer BF, Jr., Dyke SJ, Sain MK and Carlson JD (1997), "Phenomenological Model of a Magnetorheological Damper," *Journal of Engineering Mechanics*, **123**(3): 230–238.

Yang JN and Agrawal AK (2002), "Semi-active Hybrid Control Systems for Nonlinear Buildings Against Near-field Earthquakes," *Engineering Structures*, **24**: 271–280.

Yang JN *et al*. (1996), "Control of Sliding-isolated Buildings Using Sliding-mode Control," *Journal of Struct. Eng*., **122**(2): 179–186.